Biosensors and Bioelectronics 26 (2011) 4508–4513

Contents lists available at ScienceDirect

Biosensors and Bioelectronics

journal homepage: www.elsevier.com/locate/bios

High-performance electrochemical biosensor for the detection of total cholesterol

Asieh Ahmadalinezhad, Aicheng Chen*

Department of Chemistry, Lakehead University, 955 Oliver Road, Thunder Bay, Ontario P7B 5E1, Canada

ARTICLE INFO

Article history:
Received 12 January 2011
Received in revised form 27 April 2011
Accepted 5 May 2011
Available online 12 May 2011

Keywords:
Total cholesterol
Biosensor
Cholesterol oxidase
Cholesterol esterase
Horseradish peroxidase

ABSTRACT

We report on a highly sensitive electrochemical biosensor for the determination of total cholesterol. The novel biosensor was fabricated by co-immobilizing three enzymes, cholesterol oxidase (ChO_x), cholesterol esterase (ChE) and horseradish peroxidase (HRP), on nanoporous gold networks directly grown on a titanium substrate (Ti/NPAu/ChO_x–HRP–ChE). The morphology and composition of the fabricated nanoporous gold were characterized by scanning electron microscopy (SEM), energy-dispersive X-ray spectroscopy (EDS) and X-ray diffraction spectroscopy (XRD). The electrochemical behaviour of the Ti/NPAu/ChO_x–HRP–ChE biosensor was studied using cyclic voltammetry (CV), showing that the developed biosensor possessed high selectivity and high sensitivity (29.33 $\mu A\,mM^{-1}\,cm^{-2}$). The apparent Michaelis–Menten constant, K_M^{app} of this biosensor was very low (0.64 mM), originating from the effective immobilization process and the nanoporous structure of the substrate. The biosensor exhibited a wide linear range up to 300 $mg\,dL^{-1}$ in a physiological condition (pH 7.4), which makes it very promising for the clinical determination of cholesterol. The fabricated biosensor was further tested using real food samples margarine, butter and fish oil, showing that the biosensor has the potential to be used as a facile cholesterol detection tool in food and supplement quality control.

1. Introduction

Cholesterol is made by the liver as well as being part of a healthy dietary intake of fats. Cholesterol and triglycerides are important building blocks in the structure of cells and are used in making hormones and vitamin D, and producing energy. However, having a high total cholesterol (the sum of free cholesterol and cholesterol esters) level, particularly those of the low density lipoprotein type, can cause blood vessel damage and resulting diseases such as coronary heart disease and peripheral vascular disease. High cholesterol has also been linked to nephrosis, diabetes milletus, myxedema and jaundice. On the other hand, a low cholesterol level may result in hyperthyroidism, anaemia and maladsorption (Program, 1988). Most recent studies have shown that high cholesterol can affect macrophages which are part of the innate immune system that typically gobble up pathogens and clear away dead cells (Becker et al., 2010). The desired total plasma cholesterol for an individual is less than 5.2 mM (200 $mg\,dL^{-1}$), with a high level being considered as greater than 6.2 mM (240 $mg\,dL^{-1}$) (Program, 1988). Thus, the industrial and clinical determination of cholesterol is of great interest (Adanyi and Varadi, 2003; Aravamudhan et al., 2007a; Brahim et al., 2001; Arya et al., 2008; Lee and Park, 2010).

Electrochemical biosensors offer several distinct advantages. These devices are uniquely qualified for meeting the small size, cost effectiveness, low volume and power requirements of decentralized testing and show great promise for a wide range of biomedical and environmental applications (Wang, 2005; Kafi and Chen, 2009). In the development of electrochemical biosensor, facilitation of the electron transfer between the enzyme and the electrode is a great challenge because of the deeply embedded redox-active center of the metalloenzyme. On one hand, great efforts have been made to enhance the electron transfer in sensor design by using mediators, promoters or other special materials such as peroxidases for the construction of enzyme-based biosensors (Liu and Chen, 2005; Lu et al., 2007; Reilly and Aust, 1997). On the other hand, with the use of nanomaterials, higher sensitivity and the intimate attachment of enzymes are achievable due to the nanomaterials' high surface roughness as well as their unique physical, electronic and chemical properties (Carrara et al., 2008; Li et al., 2010; Chen and Holt-Hindle, 2010). Applications of nanostructured materials have been attracting great attention in the development of high-performance electrochemical biosensors (Saxena et al., 2011; Wisitsoraat et al., 2010; Kafi et al., 2010). Among them,

* Corresponding author. Tel.: +1 807 3438318; fax: +1 807 3467775.
E-mail address: aicheng.chen@lakeheadu.ca (A. Chen).

0956-5663/$ – see front matter © 2011 Elsevier B.V. All rights reserved.
doi:10.1016/j.bios.2011.05.011

gold nanomaterials have gained particular interest due to their ease of synthesis and functionalization, high chemical stability, low inherent toxicity (biocompatibility), and tunable optical and electronic properties (Eustis and El-Sayed, 2006; Ofir et al., 2008). It has been reported that the above mentioned properties of Au nanomaterials can effectively facilitate the electron transfer in the design of an electrochemical biosensor (Ahmadalinezhad et al., 2009; Safavi and Farjami, 2011; Sperling et al., 2008). Few biosensors have been reported for cholesterol determination compared with those reported for glucose; thus, developing biosensors based on gold nanostructures for the detection of total cholesterol may have a significant impact on both the clinical diagnostics and the food industry.

To develop the electrochemical cholesterol biosensor, Aravamudhan et al. attached the enzymes to the surface of aligned-gold nanowires through direct physical adsorption (Aravamudhan et al., 2007a). Their studies showed the fabricated biosensor with the sensitivity of 0.85 $\mu A\,mM^{-1}$ and the Michaelis–Menten constant of 17.1 mM. To improve the sensitivity, Gopalan et al. recently reported on the fabrication of a biosensor for the detection of free cholesterol by combining the advantageous features of MWNT (multi-walled carbon nanotubes), Au nanoparticles, chitosan and ionic liquid (Gopalan et al., 2009). Chitosan, a polysaccharide composed mainly of β-(1,4)-linked 2-deoxy-2-amino-D-glucopyranose units, is the deacetylated product of chitin, poly (N-acetyl-D-glucosamine). Chitosan has been used for the fabrication of biosensing devices because of its biocompatibility, biodegradability, multiple functional groups, as well as its solubility in acidic aqueous medium (Ahmadalinezhad et al., 2009; Tiwari and Gong, 2008). Given the huge medical implications, the industrial and clinical determination of cholesterol is increasingly important. Since 70% of cholesterol exists in ester form and 30% as free form in a blood sample, detection of the total cholesterol is desirable. In the present work, for the first time, we co-immobilized three enzymes, cholesterol oxidase (ChO_x), cholesterol esterase (ChE) and horseradish peroxidase (HRP), on the nanoporous Au networks with the aid of chitosan for the detection of the total cholesterol. The nanoporous Au networks were directly grown on a titanium (Ti) substrate using the hydrothermal method. The fabricated biosensor was free of any other promoters or special materials toxic to the environment and human. Our electrochemical measurements show that the fabricated cholesterol biosensor has high sensitivity, a very low Michaelis–Menten constant, a wide linear range, low detection limit, high selectivity and excellent stability. The cholesterol biosensor developed in this study was further tested using real food samples, indicating the promising applications in both clinical diagnostics and the food industry.

2. Experimental

2.1. Reagents and materials

Cholesterol oxidase (from *Streptomyces* species), cholesterol esterase (from hog pancreas), cholesterol, glucose, and Triton® X-100 (t-octylphenoxypolyethoxyethanol) were purchased from Sigma, 4-cholesten-3-on from Aldrich, titanium plates (1.25 cm × 0.8 cm × 0.5 mm, 99.2%) from Alfa Aesar and lactic acid from Fluka. Horseradish peroxidase, ascorbic acid, uric acid, lactic acid, sodium phosphate dibasic and sodium phosphate monobasic were used as received from Sigma–Aldrich. Nanopure water (18.2 MΩ cm) was used to prepare all solutions. All other chemicals were analytical grade and were used as received from commercial sources. A stock solution of cholesterol was prepared by dissolving cholesterol in isopropanol, then adding Triton X-100 and finally the phosphate buffer (pH 7.4) in a volume ratio of 10:4:86.

2.2. Preparation of the cholesterol biosensor

The hydrothermal method used in fabricating the nanoporous gold networks is similar to the previous studies (Koczkur et al., 2007; Wang et al., 2008; Peng et al., 2004). Briefly, titanium plates (1.25 cm × 0.8 cm) were washed in acetone, followed by Nanopure water, and then etched in a solution of 18 wt% hydrochloric acid at 85 °C for 10 min to remove the oxide layer and roughen the Ti surface. The etched Ti substrates were transferred into Teflon-lined autoclaves containing 10 mL of an aqueous mixture of inorganic metal precursor and a reducing agent. A 1.0 M ammonium formate solution was used as the reducing agent and the metal precursor was $HAuCl_4$. The autoclaves were sealed and heated at 180 °C for 10 h. The Ti plates coated with Au were dried and annealed under argon at 250 °C for 2 h. After final rinsing with pure water, the Ti plates coated with nanoporous gold were ready for further surface analysis and for the immobilization of enzymes. To immobilize the enzymes, a mixture of 20 μL of 2 mg mL^{-1} of cholesterol oxidase (ChO_x), 10 μL of 2 mg mL^{-1} horseradish peroxidise (HRP), 10 μL of 2 mg mL^{-1} of cholesterol esterase (ChE) and 10 μL of 2 mg mL^{-1} of chitosan was cast onto the nanoporous Au electrode (Ti/NPAu/ChO_x–HRP–ChE). Chitosan was used as a glue to enhance the stability of the biosensor (Khan and Dhayal, 2008). All prepared biosensors were stored at 4 °C when not in use.

2.3. Instruments and electrochemical experiments

Surface morphology and composition of the synthesized samples were characterized using scanning electron microscopy (SEM) (JEOL JSM 5900LV) equipped with an energy-dispersive X-ray spectrometer (EDS) (Oxford Links ISIS). Surface elemental compositions based on quantitative EDS analysis were reported in average values of readings taken at five different spots on each sample surface. All electrochemical experiments were performed using an electrochemical workstation (CHI660B, CH instrument Inc.), connected with an in-house-built, three-electrode glass cell (30 mL). A platinum coil was used as a counter electrode and was flame-annealed before each experiment. An Ag/AgCl (saturated KCl) electrode was used as the reference electrode. The fabricated Ti/NPAu/ChO_x–HRP–ChE electrodes were used as the working electrode. All potentials reported in this paper are referred to the Ag/AgCl (saturated KCl) reference electrode. Cyclic voltammetric measurements of cholesterol were carried out in a 0.1 M phosphate buffer solution (pH 7.4) at selected potential ranges. All measurements were conducted in a 30 mL solution and at room temperature (22 ± 2 °C).

3. Results and discussion

3.1. Surface morphological studies

Fig. 1A and B present a typical SEM image and EDS spectrum of the nanoporous gold (Ti/NPAu) electrode, respectively, fabricated using the hydrothermal method. The SEM image shows that nanoporous gold structure was formed and covered the substrate and that the thickness of the nanoporous gold layer was around 0.4 μm estimated from the depth of the pores. The diameter of the formed randomly porous structures varies from tens to hundreds of nanometers. Only Au and Ti peaks appear in the EDS spectrum, and no discernible carbon or oxygen signals are seen in the figure, showing that the synthesized nanoporous Au is free of surface organic impurities. The XRD pattern of the as-synthesized Ti/NPAu surface is shown in Fig. 1C. All diffraction peaks originate from the Au film and the Ti substrate. The lattice constant calculated from the pattern was 4.079 Å, consistent with the litera-

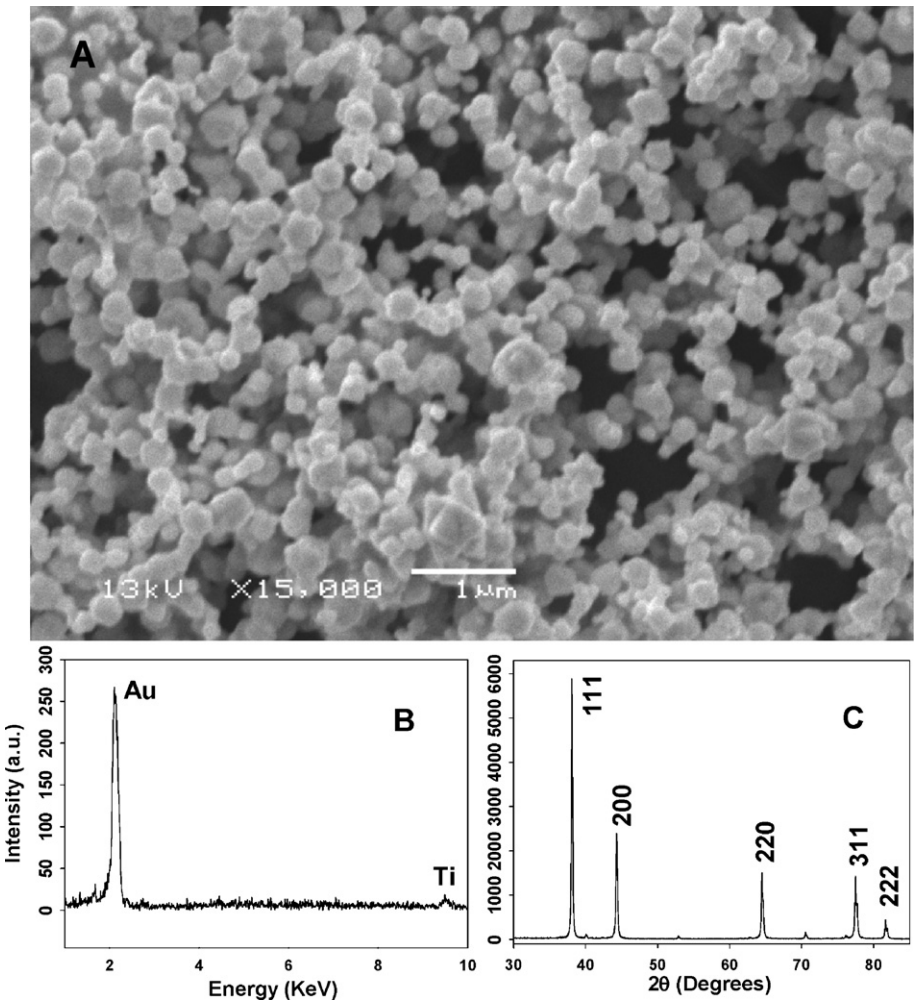

Fig. 1. (A) SEM image of the nanoporous Au directly grown on a titanium substrate. (B) EDS spectrum of the synthesized nanoporous Au. (C) XRD spectrum recorded from the synthesized nanoporous Au.

ture $a = 4.078$ Å (Joint Committee on Powder Diffraction Standards file no. 04-0784). The XRD analysis reveals that the agglomerated structure observed by SEM has an average crystallite size of 22 nm. As seen in Section 2, only inorganic metal precursors and diluted reducing agent were involved in the direct growth of nanoporous Au on the Ti substrate. To determine the electrochemical active surface area, we recorded CV curves of the nanoporous Au electrode and a smooth polycrystalline Au electrode in 0.5 M H_2SO_4, revealing that the roughness factor of the nanoporous Au electrode is 5.9. The above results show that the one-step hydrothermal reduction process is an environmentally friendly approach and does not require any further separation and purification of the formed nanoporous Au with a large surface area, which is ready for the immobilization of enzymes.

3.2. Electrochemical characterization

The electrochemical responses of the Ti/AuNPs/ChO_x–HRP–ChE electrodes were studied by cyclic voltammetry. Fig. 2A shows the bioelectrocatalytic behaviour of the enzyme electrode recorded in a phosphate buffer solution (pH 7.4) in the potential range of −0.8 to 0.4 V at different scan rates. For instance, at the scan rate of 50 mV s^{-1}, the cathodic and anodic peaks appear at −0.36 and −0.047 V, respectively. The formal potential, $E^0 = 1/2\ (E_{p,a} + E_{p,c})$, was calculated to be −0.203 V (*vs.* Ag/AgCl) and the electroactive enzyme amount, $\Gamma = Q/nFA$, (Where Q is the integrated charge which is calculated based on the peak area under the I–E curve, n is the electron number transferred, F the faraday constant, and A is the geometric surface area of the working electrode) is 2.1×10^{-9} mol cm^{-2}. This is higher than the experimental values 7.52×10^{-10} (Deng et al., 2010) and 4.7×10^{-10} mol cm^{-2} (Deng et al., 2009) for the monolayer of flavoenzymes reported in literature. The higher value can be ascribed to the efficient immobilization of the enzymes on the nanoporous gold surface with high conductivity and a large surface area.

As seen in Fig. 2B, both the anodic and cathodic peak currents increase linearly with the scan rates, indicating that the pair of redox waves originates from the surface confined molecules. The anodic and cathodic peak potentials also change as a function of the scan rate (10–300 mV s^{-1}). With increasing the scan rate, the oxidation peak shifts to more positive potentials, while the reduction peak shifts to more negative potentials. The anodic and cathodic peak potentials are linearly dependent on the logarithm of the scan rates (ν) when $\Delta E_p > 200/n$ where n is the number of electron transferred. This is in agreement with Laviron theory (Laviron, 1979; Zhang et al., 2005). The plots of E_p *vs.* $\log \nu$ are displayed in Fig. 2C, yielding two straight lines with slopes of $-2.3RT/\alpha nF$ and $2.3RT/(1-\alpha)nF$ for the cathodic and anodic peaks, respectively. Thus, experimental α was estimated to be 0.36.

The effect of pH on the performance of the Ti/NPAu/ChO_x–HRP–ChE electrodes was investigated in 0.1 M phosphate buffer solutions with the pH varied from 4.0 to 9.0 at

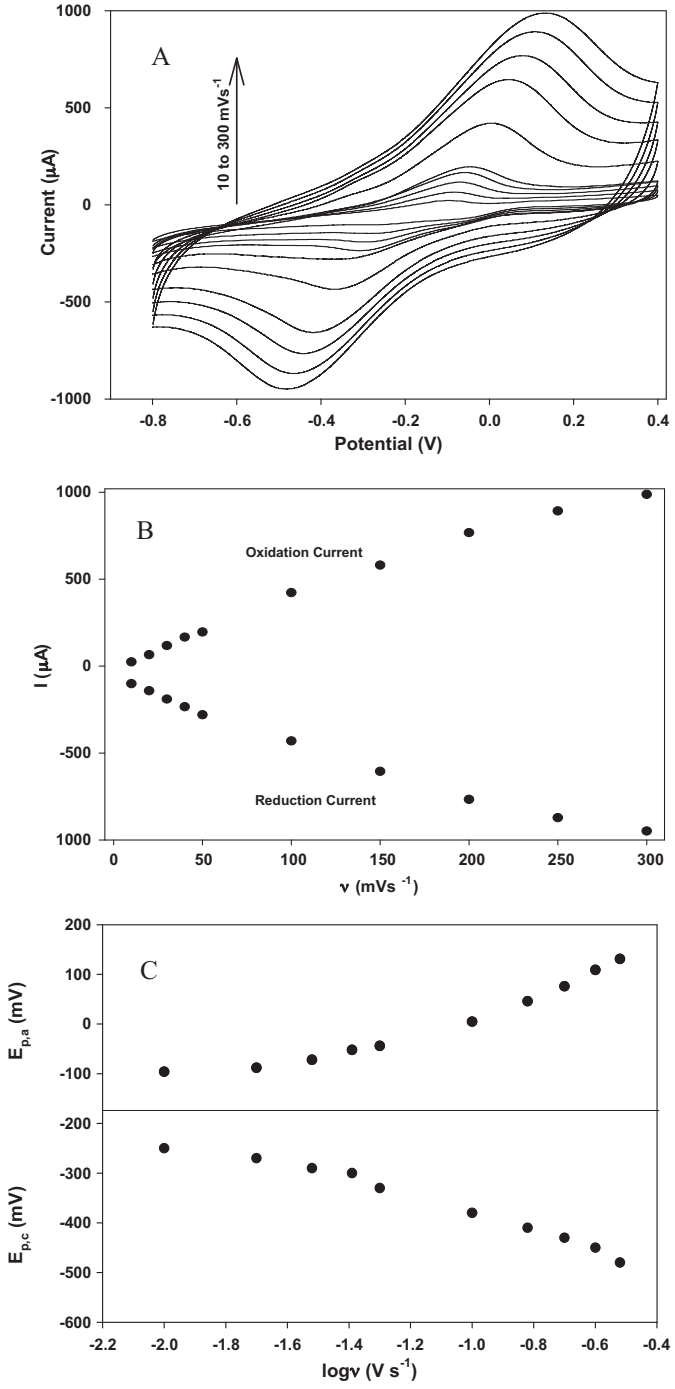

Fig. 2. (A) Cyclic voltammamograms of the Ti/AuNPs/ChO_x–HRP–ChE electrode at different scan rates (10, 20, 30, 40, 50, 100, 150, 200, 250, 300 m Vs^{-1}) in a phosphate buffer (pH 7.4). (B) Plot of anodic and cathodic peak currents *vs.* scan rates. (C) Variation of peak potentials *vs.* the logarithm of the scan rates.

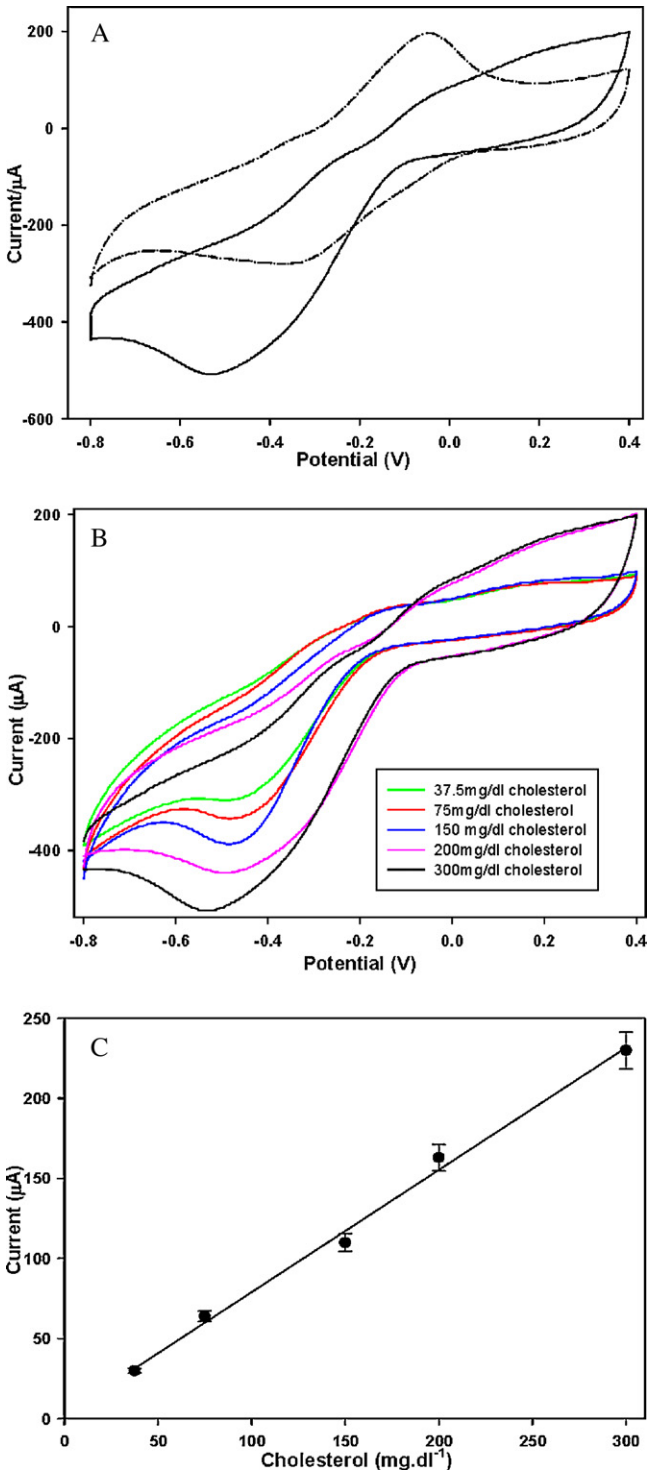

Fig. 3. (A) Cyclic voltammetric response of the Ti/AuNPs/ChO_x–HRP–ChE electrode measured in a phosphate buffer (pH 7.4) in the absence (dashed line) and presence (solid line) of cholesterol 300 mg dL^{-1}, (B and C) Cyclic voltammograms and calibration curve of the biosensor upon addition of different concentrations of cholesterol in a phosphate buffer (pH 7.4). Potential scan rate: 50 mV s^{-1}.

the scan rate of 50 m Vs^{-1}. The current response was found to be maximum at pH 7–8, indicating that the biosensor is more active at this pH range and the immobilized enzymes retain their natural structure and do not denature. Thus, all the performance tests of the biosensor were conducted at pH 7.4 to simulate the physiological condition.

Fig. 3A presents the two CV curves of the Ti/NPAu/ChO_x–HRP–ChE electrode recorded in a phosphate buffer solution (pH 7.4) in the absence of cholesterol (dashed line) and in the presence of 300 mg dL^{-1} cholesterol (solid line). Comparison of the two CV curves shows that the addition of cholesterol decreased the anodic current and significantly increased the cathodic current, revealing the strong response of the Ti/AuNPs/ChO_x–HRP–ChE electrode to cholesterol. As seen in Fig. 3B, the reduction peak current increased strongly with the increase of the concentration of cholesterol, illustrating a typical electrocatalytic reduction process of H_2O_2 produced by the enzymatic reaction of cholesterol with

Table 1
Comparison of the performances of various types of gold-based cholesterol biosensors.

Electrode	K_m (mM)	Sensitivity ($\mu A\,mM^{-1}$)	Linearity (mM)	Durability	Reference
DTSP–Au/ChO_x	N/A	0.054	0.2–2.1	40 days, 77%	Parra et al. (2007)
(MWNTs)–Au/PPD–ChO_x	7.17	0.559	0.5–6	N/A	Guo et al. (2004)
MWNT(SH)–Au/Chi–IL/ChO_x	N/A	0.2	0.5–5	20 days, 80%	Gopalan et al. (2009)
Au Nanowire/ChO_x–ChE	17.1	0.85	0.01–0.060	10 days, 75%	Aravamudhan et al. (2007b)
Ti/NPAu/ChO_x–HRP–ChE	0.64	29.33	0.97–7.8	60 days, 95%	This work

ChO_x: Cholesterol oxidase, ChEt and ChE: Cholesterol esterase, DTSP: dithiobissuccinimidyl propionate, Au: Gold, MWNT: Multi-wall carbon nanotubes, Chi: Chitosan, IL: Ionic liquid, NPAu: Nanoporous gold, HRP: Horseradish peroxidase, PPD: poly(o-phenylenediamine)

cholesterol oxidase on the biosensor surface area as the following mechanism (Aravamudhan et al., 2007b; Volonte et al., 2010):

$$\text{Cholesterol} + O_2 \xrightarrow{ChO_x} \text{Cholest} - 4 - \text{en} - 3 - \text{one} + H_2O_2 \quad (1)$$

$$\text{Cholesterol ester} + H_2O \xrightarrow{ChE} \text{Cholesterol} + \text{Fatty acids} \quad (1^*)$$

Cholesterol oxidase is an alcohol dehydrogenase/oxidase flavoprotein that catalyzes the dehydrogenation of C(3)–OH of a cholesterol molecule to yield the corresponding carbonyl product. During the reductive half-reaction, the oxidized FAD (flavin adenine dinucleotide) cofactor accepts a hydride from the substrate and, in the ensuing oxidative half-reaction, the reduced flavin transfers the redox equivalents to molecular oxygen yielding hydrogen peroxide. Interestingly, the carbonyl species can also catalyze the isomerization of cholest-5-en-3-one (the product of the redox reaction) to cholest-4-en-3-one (Aravamudhan et al., 2007b). While the immobilized ChO_x catalyzes the oxidation of cholesterol, the ChE catalyzes the hydrolysis of esterase-esterified cholesterol, thus allowing us to determine the total cholesterol (Shih et al., 2009).

To sense the formed H_2O_2 in Eq. (1) electrochemically, either a reducing or oxidising agent is required. Peroxidases such as HRP are ubiquitous oxidative heme-containing enzymes with which, in an early step in the catalytic cycle, H_2O_2 binds to the heme in the Fe(III) state. This binding causes the heterolytic cleavage of the oxygen–oxygen bond of H_2O_2 (Rodriguez-Lopez et al., 2001).

$$H_2O_2 + \text{HRP(Fe(III))} \rightarrow \text{Compound I (Fe(IV)} = \text{O)} + H_2O \quad (2)$$

$$\text{Compound I(Fe(IV)} = \text{O)} \rightarrow \text{Compound II(Fe(IV)} = \text{O)} \quad (3)$$

$$\text{Compound II(Fe(IV)} = \text{O)} \rightarrow \text{HRP(Fe(III))} + H_2O \quad (4)$$

A water molecule is released during this reaction with the concomitant two-electron oxidation of the heme to form an intermediate (compound I) comprising a ferryl species (Fe(IV)=O) and a porphyrin radical cation (Courteix and Bergelt, 1995). Compound I is then converted back to the resting enzyme via two successive single-electron transfers from the reducing substrate molecules. The first reduction of the porphyrin radical cation yields a second enzyme intermediate, compound II, which retains the heme in the ferryl (Fe(IV)=O) state (Dunford and Stillman, 1976). Compound II oxidizes an additional equivalent of substrate, generating ferric enzyme and the corresponding substrate free radical (Reilly and Aust, 1997). As seen in Fig. 3C, the cyclic voltammetric response of the Ti/NPAu/ChO_x–HRP–ChE biosensor to different concentrations of cholesterol solutions shows a linear dynamic range of up to 300 mg dL^{-1} and sensitivity of 29.33 $\mu A\,mM^{-1}\,cm^{-2}$. Although it is difficult to determine the exact response time of the biosensor, the CV curves were recorded at the scan rate of 50 m Vs^{-1}, indicating that the response of the biosensor is fast. Five biosensors constructed independently gave a relative standard deviation (R.S.D.) of 5.0%. The detection limit of the biosensor was estimated to be 0.5 mg dL^{-1}. Since the desired total plasma cholesterol for an individual is less than 5.2 mM (200 mg dL^{-1}), with a high level being considered as greater than 6.2 mM (240 mg dL^{-1}), the fabricated biosensor covers a wide range of cholesterol concentration, promising for the clinical diagnostics of total cholesterol.

The apparent Michaelis–Menten constant (K_M^{app}), which gives an indication of the enzyme–substrate kinetics, can be estimated from the Lineweaver–Burk equation (Kamin and Wilson, 1980):

$$\frac{1}{I_{ss}} = \left(\frac{K_M^{app}}{I_{max}}\right)\left(\frac{1}{C}\right) + \frac{1}{I_{max}} \quad (5)$$

where I_{ss} is the steady state current, I_{max} is the current measured for the enzymatic product when electrode surface is saturated and C is the concentration of cholesterol. From the Lineweaver–Burk equation, the apparent Michaelis–Menten constant of the Ti/NPAu/ChO_x–HRP–ChE biosensor was calculated to be 0.64 mM, which is much lower than the cholesterol biosensors reported in literature (Table 1). The small K_M^{app} value indicates that the immobilized enzymes possess high enzymatic activity and that the fabricated biosensor exhibits a high affinity for cholesterol.

3.3. Selectivity and long-term stability of the biosensor

We further tested the selectivity of the Ti/NPAu/ChO_x–HRP–ChE biosensor using four common interfering species. Fig. 4 presents the response of the Ti/NPAu/ChO_x–HRP–ChE biosensor to 0.1 mM

Table 2
Cholesterol detection of real samples by the Ti/AuNPs/ChO_x–HRP–ChE biosensor.

Samples	AuNPs biosensor (mg)	Product label (mg)	Brand
Margarine	0.69 ± 0.05	0	NoName
Organic Butter	2.35 ± 0.03	2.4	Harmoie
Fish oil	45.82 ± 0.06	46	Naturaceutical Science Institute

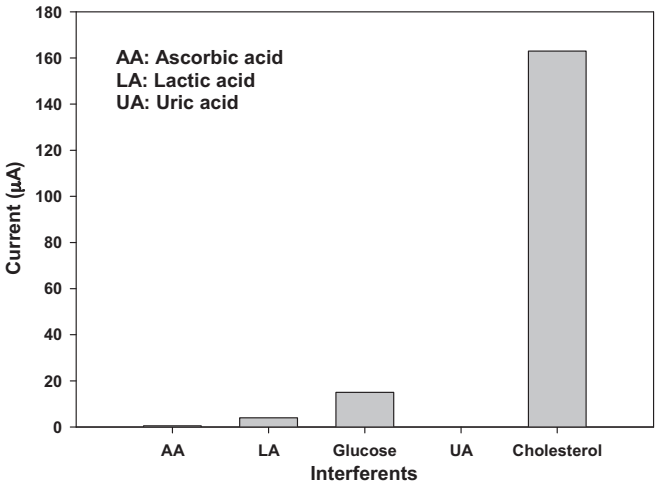

Fig. 4. Selectivity response of the Ti/NPAu/ChO_x–HRP–ChE electrode after the addition of ascorbic acid (0.1 mM), lactic acid (5 mM), glucose (5 mM), uric acid (0.1 mM) and finally cholesterol (5.2 mM) into a phosphate buffer (pH 7.4) individually (background current was subtracted).

ascorbic acid, 5 mM lactic acid, 5 mM glucose, 0.1 mM uric acid and 5.2 mM cholesterol in 0.1 M PBS (pH 7.4). The biosensor produces negligible current signals for lactic acid and uric acid, a small response to ascorbic acid and glucose, but a very strong response to cholesterol.

The stability of the Ti/NPAu/ChO_x–HRP–ChE biosensor was tested by measurement of a 200 mg dL^{-1} standard cholesterol solution for 60 days. The tests were carried out once a week. During this period, the biosensors were stored in a phosphate buffer solution at 4 °C. The biosensor exhibited 95% of the initial current response after the 60 day period. The high stability can be attributed to the use of chitosan and the nanoporous Au networks. Since chitosan in an aqueous solvent is protonated and positively charged, it can be strongly adsorbed onto the nanoporous gold networks. The resulting interaction between gold–chitosan increases the retention of enzymes on the surface. In addition, gold nanostructures can strongly adsorb enzymes and prevent the leakage of the immobilized enzymes (Luo et al., 2004). The high sensitivity and high stability of the fabricated biosensor indicate that the nanoporous Au network structure along with chitosan provides an excellent microenvironment for the immobilization of the enzymes.

3.4. Real sample analysis

The developed Ti/NPAu/ChO_x–HRP–ChE biosensor was further tested using real food samples butter, margarine and fish oil. The real samples were prepared using the same procedure as the cholesterol solution described in Section 2.1. The Margarine sample, which contains only vegetable fat, showed a small signal. As seen in Table 2, the amount of total cholesterol found in butter, margarine and fish oil was 2.35, 0.69 and 45.82 mg, respectively. This is in good agreement with the amount of the total cholesterol listed on the product labels (2.4, 0 and 46 mg for Organic butter, NoName margarine and Naturaceutical Science Institute fish oil, respectively). All these results show that the fabricated cholesterol biosensor offers a great potential of application in cholesterol quality control of food products.

4. Conclusions

We have successfully fabricated a novel high-performance cholesterol biosensor by co-immobilizing cholesterol oxidase, cholesterol esterase and horseradish peroxidase on the nanoporous gold networks. The immobilized cholesterol oxidase effectively catalyzes the oxidation of cholesterol while the cholesterol esterase catalyzes the hydrolysis of esterase-esterified cholesterol, thus allowing the determination of the total cholesterol. Meanwhile, the immobilized horseradish peroxidase facilitates the detection of the H_2O_2 generated by the catalytic conversion of cholesterol to cholest-4-en-3-one. The developed Ti/NPAu/ChO_x–HRP–ChE biosensor showed highly anti-interferents behaviour as tested toward common interfering species such as ascorbic acid, uric acid, lactic acid and glucose. A very low Michaelis–Menten constant indicates a very high activity of the immobilized enzymes. Under the physiological condition (pH 7.4), the designed biosensor exhibited reliable cyclic voltammetric responses, high sensitivity, a wide linear range up to 300 mg dL^{-1} and very high stability. The developed biosensor was also successfully used to measure the total cholesterol in real food samples. The high-performance along with the ease of fabrication and low costs makes the new Ti/NPAu/ChO_x–HRP–ChE biosensor promising for the detection of total cholesterol in both clinical diagnostics and the food industry.

Acknowledgments

This work was supported by a Discovery Grant from the Natural Sciences and Engineering Research Council of Canada (NSERC). A. Chen acknowledges NSERC and the Canada Foundation for Innovation (CFI) for a Canada Research Chair Award.

References

Adanyi, N., Varadi, M., 2003. Eur. Food Res. Technol. 218, 99–104.
Ahmadalinezhad, A., Kafi, A.K.M., Chen, A., 2009. Electrochem. Commun. 11, 2048–2051.
Aravamudhan, S., Kumar, A., Mohapatra, S., Bhansali, S., 2007a. Biosens. Bioelectron. 22, 2289–2294.
Aravamudhan, S., Ramgir, N.S., Bhansali, S., 2007b. Sens. Actuators B 127, 29–35.
Arya, S.K., Datta, M., Malhotra, B.D., 2008. Biosens. Bioelectron. 23, 1083–1100.
Becker, L., Gharib, S.A., Irwin, A.D., Wijsman, E., Vaisar, T., Oram, J.F., Heinecke, J.W., 2010. Cell Metab. 11, 125–135.
Brahim, S., Narinesingh, D., Guiseppi-Elie, A., 2001. Anal. Chim. Acta 448, 27–36.
Carrara, S., Shumyantseva, V.V., Archakov, A.I., Samori, B., 2008. Biosens. Bioelectron. 24, 148–150.
Chen, A., Holt-Hindle, P., 2010. Chem. Rev. 110, 3767–3804.
Courteix, A., Bergelt, A., 1995. Enzyme Microb. Technol. 17, 1087–1093.
Deng, C., Chen, J., Nie, Z., Si, S., 2010. Biosens. Bioelectron. 26, 213–219.
Deng, S., Jian, G., Lei, J., Hu, Z., Ju, H., 2009. Biosens. Bioelectron. 25, 373–377.
Dunford, H.B., Stillman, J.S., 1976. Coord. Chem. Rev. 19, 187–251.
Eustis, S., El-Sayed, M.A., 2006. Chem. Soc. Rev. 35, 209–217.
Gopalan, A.I., Lee, K.-P., Ragupathy, D., 2009. Biosens. Bioelectron. 24, 2211–2217.
Guo, M., Chen, J., Li, J., Nie, L., Yao, S., 2004. Electroanalysis 16, 1992–1998.
Kafi, A.K.M., Ahmadalinezhad, A., Wang, J., Thomas, D.F., Chen, A., 2010. Biosens. Bioelectron. 25, 2458–2463.
Kafi, A.K.M., Chen, A., 2009. Talanta 79, 97–102.
Kamin, R.A., Wilson, G.S., 1980. Anal. Chem. 52, 1198–1205.
Khan, R., Dhayal, M., 2008. Electrochem. Commun. 10, 263–267.
Koczkur, K., Yi, Q., Chen, A., 2007. Adv. Mater. 19, 2648–2652.
Laviron, E., 1979. J. Electroanal. Chem. 101, 19–28.
Lee, Y.J., Park, J.Y., 2010. Biosens. Bioelectron. 26, 1353–1358.
Li, Y., Bai, H., Liu, Q., Bao, J., Han, M., Dai, Z., 2010. Biosens. Bioelectron. 25, 2356–2360.
Liu, S., Chen, A., 2005. Langmuir 21, 8409–8413.
Lu, X., Zou, G., Li, J., 2007. J. Mater. Chem. 17, 1427–1432.
Luo, X.-L., Xu, J.-J., Du, Y., Chen, H.-Y., 2004. Anal. Biochem. 334, 284–289.
Ofir, Y., Samanta, B., Rotello, V.M., 2008. Chem. Soc. Rev. 37, 1814–1825.
Parra, A., Casero, E., Pariente, F., Vázquez, L., Lorenzo, E., 2007. Anal. Bioanal. Chem. 388, 1059–1067.
Peng, X., Koczkur, K., Nigro, S., Chen, A., 2004. Chem. Commun. 24, 2872–2873.
Program, N.C.E., 1988. Arch. Intern. Med. 148, 36–69.
Reilly, C.A., Aust, S.D., 1997. Chem. Res. Toxicol. 10, 328–334.
Rodriguez-Lopez, J.N., Lowe, D.J., Hernandez-Ruiz, J., Hiner, A.N.P., Garcia-Canovas, F., Thorneley, R.N.F., 2001. J. Am. Chem. Soc. 123, 11838–11847.
Safavi, A., Farjami, F., 2011. Biosens. Bioelectron. 26, 2547–2552.
Saxena, U., Chakraborty, M., Goswami, P., 2011. Biosens. Bioelectron., doi:10.1016/j.bios.2010.12.009.
Shih, W.C., Yang, M.C., Lin, M.S., 2009. Biosens. Bioelectron. 24, 1679–1684.
Sperling, R.A., Gil, P.R., Zhang, F., Zanella, M., Parak, W.J., 2008. Chem. Soc. Rev. 37, 1896–1908.
Tiwari, A., Gong, S., 2008. Electroanalysis 20, 2119–2126.
Volonte, F., Pollegioni, L., Molla, G., Frattini, L., Marinelli, F., Piubelli, L., 2010. BMC Biotechnol. 10, 33.
Wang, J., 2005. Analyst 130, 421–426.
Wang, J., Thomas, D.F., Chen, A., 2008. Anal. Chem. 80, 997–1004.
Wisitsoraat, A., Sritongkham, P., Karuwan, C., Phokharatkul, D., Maturos, T., Tuantranont, A., 2010. Biosens. Bioelectron. 26, 1514–1520.
Zhang, L., Jiang, X., Wang, E., Dong, S., 2005. Biosens. Bioelectron. 21, 337–345.